

Document downloaded from:

<http://hdl.handle.net/10251/140183>

This paper must be cited as:

Vega, J.; Andrio, A.; Lemus, A.; Díaz, J.; Del Castillo, L.; Gavara, R.; Compañ Moreno, V. (01-0). Modification of polyetherimide membranes with ZIFs fillers for CO₂ separation. Separation and Purification Technology. 212:474-482.
<https://doi.org/10.1016/j.seppur.2018.11.033>



The final publication is available at

<https://doi.org/10.1016/j.seppur.2018.11.033>

Copyright Elsevier

Additional Information

Modification of polyetherimide membranes with ZIFs fillers for CO₂ separation

Vega J.¹, Andrio A.², Lemus A.A.¹, Díaz J.A.I.¹, del Castillo L.F.³, Gavara R.⁴, *Compañ V.⁴

¹Centro de Investigación en Ciencia Aplicada y Tecnología Avanzada, Unidad Legarí, Instituto Politécnico Nacional, CDMX, México.

²Departamento de Física, Escuela Superior de Tecnología y Ciencias Experimentales, Universidad Jaime I, 12072 Catellón, Spain.

³Departamento de Polímeros, Instituto de Investigaciones en Materiales, Universidad Nacional Autónoma de México (UNAM), Ciudad Universitaria, C. P. 170-360, Coyoacán, México DF, 04510

⁴Food Safety and Preservation Department, IATA-CSIC, Avda. Agustín Escardino 7, 46980 Paterna, Valencia Spain.

⁵Departamento de Termodinámica Aplicada, ETSII, Universidad Politécnica de Valencia, Campus de Vera s/n, 46022 Valencia, Spain.

Abstract

Flat hybrid membranes composed of polyetherimide (PEI) as matrix and zeolitic imidazolate frameworks (ZIFs) as fillers at concentrations of 10 and 20 wt % were prepared. Apparent permeability coefficient and apparent diffusivity coefficient of gases (CO₂ and N₂) for these hybrid membranes (PZIFs) were determined by the “time-lag” method. The experimental conditions used were from 25 °C to 55 °C with pressures of 2, 3 and 5 bar. The PZIFs with fillers of ZIF-8 (PZ-Zn) and ZIF-67 (PZ-Co) showed apparent selectivities ($\alpha_{P_a(\text{CO}_2)/P_a(\text{N}_2)}$) of 39.6 and 27.5, respectively, higher than the $\alpha_{P_a(\text{CO}_2)/P_a(\text{N}_2)}$ of the reference membrane PEI, while the membrane with filler of ZIF-Mix (PZ-Zn/Co) showed the lowest $\alpha_{P_a(\text{CO}_2)/P_a(\text{N}_2)}$ selectivity of 10.3 in the membrane series (under conditions of 25 °C and 2 bar). It is proposed that the selectivity of the membrane series can be attributed to two critical factors: the particle size/distribution ratio in the polymer base and sorption of CO₂ at local sites of the bimetallic mixture.

On the other hand, gas permeation studies (O₂, CO₂ and CH₄, and CO₂/CH₄ and CO₂/C₂H₄ mixtures), were carried out in the series of PZIFs membranes. Permeability data were obtained by an isostatic method based on a permeation cell connected in series to a gas chromatograph where the rate of permeated gases was analyzed until a stationary state was reached. The complementary characterization techniques were: scanning electron microscopy, thermogravimetric analysis, and powder X-ray diffraction, which support the existence of the amorphous/crystalline phases of the PZIFs.

Keywords: Zeolitic Imidazolate Frameworks, Mixed Matrix Membranes, PZIFs, permeability.

1. Introduction

Membrane technology is an attractive and competitive alternative with regard to technologies (for example: separation of gases with amines and reforming of methane with water vapor), which are focused on related processes in obtaining energy and capturing and / or separation of greenhouse gases (especially CO₂ and CH₄), which are mostly released into the environment and promote the very well-known global warming. [1] In the last decade, the introduction of polymer membranes in gaseous separation processes, hydrogen recovery (H₂ / HC), sweetening of natural gas (CO₂ / CH₄), adjustment of the ratio of synthesis gas or fuel cells (H₂ / CO₂), among others, has had an increasing interest due to its multiple benefits, such as: low surface area of operation, assembly of units by modules, low operating costs, the non-use of chemical additives, etc. [2,3] Currently most of the gas separation studies carried out on polymer membranes, [1] asymmetric membranes, [4] and composite membranes, [5] seem to be oriented towards the use of materials such as molecular sieves, where the ratio of pore size / kinetic diameter (polymer / gas, respectively) points to being the predominant factor before the permeation and gas separation. However, another factor that participates in the gas transportation and that has not yet been much studied is the adsorbate-adsorbent sorption process, which can play an important role in the separation of gases in the membrane technology. Today there is a great interest in the research and development of new membrane structures whose objective is to obtain greater selectivity and permeability of specific gases. The polyetherimide (PEI), commercially known as ULTEM[®], is a high performance thermoplastic polymer with imide, isopropylidene and ether groups [6]. The repeating unit of PEI is [C₃₇H₂₄O₆N₂]_n with molecular weight of 592 g/mol. The polymer presents glass transition temperature at 215 °C, and decomposition temperature at 427 °C [6,7]. These features make it interesting for high temperature applications. Zeolitic Imidazolate Frameworks (ZIFs), are members of a new class of organic-inorganic hybrid materials called Metal Organic Frameworks (MOFs), which offer diversity of architectures, pore sizes and high surface areas [8,9]. ZIFs have been used as fillers in polymeric matrices in membrane technology due to its great potential for sorption, separation of mixtures of gases and vapors [10,11,12,13]. ZIF-8, which molecular formula is: Zn (mIm)₂, (where mIm=2-methylimidazole) has sodalite topology and shows adsorption affinity CO₂ molecules; also the ZIF-8 exhibits exceptional thermal and chemical stability

[8,14,15]. ZIF-67, Co (mIm)₂, ZIF-Mix, Zn/Co (mIm)₂, and ZIF-8 are isostructural materials exhibit six members rings (~ 3.4 Å) as pore openings [16,17,18]. These three materials have shown a differentiated sorption performance (when studied by IGC), due to the charge anisotropy, consequence of the metallic center nature. It seems likely that this behavior would be reproducible employing ZIFs as fillers in the polymeric base PEI.

In the present work, it is proposed that the variation of the permeation coefficients obtained not only depends on the ratio of pore size/kinetic diameter of the gas, but also on the factors such as the isotropy and anisotropy of the electrical charge that are present in each of the ZIFs structures and the dipole moment of the gas in question. So, mixed-matrix flat membranes composed of microporous fillers (ZIF-8, ZIF-67 and the bimetallic mixture ZIF-Zn / Co) and the polymeric PEI base were prepared. The pure gas permeation coefficients and gas mixture separation were evaluated for the series of membranes obtained. In addition, the materials obtained were studied by means of DRX, SEM, and TGA to demonstrate the presence of the microporous phase in the polymeric base and to analyze the thermal stability of the obtained membranes.

2. Experimental

2.1. Materials

Polyetherimide, PEI was purchased from Sabic. N-methyl-2-pyrrolidone ($\geq 99.7\%$), NMP; 2-methylimidazole (99%), 2-mIm; and zinc chloride ($\geq 97\%$), ZnCl₂ were purchased from Sigma Aldrich. Cobalt chloride ($\geq 99.8\%$), CoCl₂ and sodium formate ($\geq 99\%$), NaCOOH were purchased from Baker Analyzed and Reasol, respectively. Dry CO₂ and CH₄, and CO₂/CH₄ 50/50, CH₄/C₂H₄ 50/50 mixtures were supplied by Abello-Linde (Puzol, Spain).

2.2. Synthesis of ZIF-8

ZIF-8 (Z-Zn) was synthesized in our laboratory according to the procedure reported elsewhere. [8]. In brief, the mixture of 821 mg of 2-mIm and 765 mg of NaCOOH in 30 ml of methanol was placed under stirring for 20 min. In a separate beaker a solution of 512 mg of ZnCl₂ in 15 ml of methanol was prepared. Both solutions were mixed and stirred for 25 min. Then the resulting mixture was retorted in a PTFE coated stainless steel reactor at

130°C for 4 h. The final product was centrifuged and the precipitate was washed, centrifuged and dried under vacuum for 12h.

2.3. Synthesis of ZIF-67 y ZIF-Mix

The synthesis of ZIF-67 (Z-Co) and ZIF-Mix (Z-Zn/Co) is similar to that described above: for the synthesis of Z-Co, substituting 483 mg of CoCl₂, instead of ZnCl₂. In the case of Z-Zn/Co, equimolar amounts of metal ions (Zn/Co) were used with the aim of promoting a solid solution with metal ratio of 1:1.

2.4. Preparation of colloids and membranes

PEI:NMP solutions (in 1:3 w/w relation) were mixed to form a solution. Each ZIF was added to the polymer solution at concentrations of 10 wt % and 20 wt % of the final solid product (See equation 1). The mixtures were capped and placed in an ultrasonic bath for 2 hour and then stirred during 15min. After two cycles, membranes were prepared by the casting technique; the colloidal dispersions were spread on a flat glass and placed in an oven where samples were heated from room temperature to 210°C (heating rate = 30°C/h) and kept isothermally for 2 h. The obtained hybrid membranes, PEI/ZIFs or PZIFs, (100 ± 18 µm thick) were labeled as PZ-Zn (PEI/Z-Zn), PZ-Co (PEI/Z-Co) and PZ-Zn/Co (PEI/Z-(Zn/Co)). The PZIFs membranes and PEI membrane were sealed and stored until further use.

$$\text{weight ZIF \%} = \frac{\text{weight ZIF}}{\text{weight ZIF} + \text{weight PEI}} \times 100\% \quad (\text{Eq. 1})$$

2.5. X-ray diffraction analysis

The XRD pattern of the synthesized fillers and membranes were collected using a Bruker-AXD D8-Advance diffractometer with Bragg-Brentano theta/theta geometry, with Cu, diffracted beam monochromator and scintillation detector.

2.6. Porosity analysis

The N₂ adsorption isotherms were recorded at 77 K with an ASAP 2050 pressure sorption analyzer (from Micrometrics) equipped with a Smart Vac degassing system. The processing of the adsorption data was done to obtain the surface areas (BET) and the volume of

micropores. The sample was activated under vacuum at 100 °C for 2 hours before the thermogravimetric analysis

2.7. Scanning electron microscopy

The surface morphology of the samples: ZIFs fillers and PZIFs membranes was studied using a field scanning electron microscope (JEOL 7001F EDX-WDX Oxford, INCA 350 / Wave 200). The samples were gold coated and conserved under vacuum before SEM observations.

2.8. Thermogravimetric analysis

The thermal stability of the membranes was evaluated with a TGA 2950 thermogravimetric analyzer TA Instruments (New Castle, DE, USA) by heating the sample from 25°C until 700 °C at a heating rate of 5°C/min. The experiments were carried out under nitrogen atmosphere with 60 ml/min flux.

2.9. Apparent permeability of gases

The gas permeation properties were determined by means of automated gas permeation equipment (see diagram in supporting information) and the variable-volume pressure-constant method [19]. Measuring devices used were: (PFEIFFER) Vacuum pressure sensors with ranges of 1×10^{-3} mbar in the lower chamber, 1bar in the upper chamber and a Dual Gauge TM transducer (TPG 252-A model). Gas transport gas through dense membranes is usually expressed in terms of the apparent permeability, P_a and the apparent diffusion coefficient, D_a . The apparent permeability coefficient in the steady-state may be determined by the following expression [20]:

$$P_a = \frac{273}{76} \cdot \frac{V \cdot L}{A \cdot T \cdot p_0} \cdot \frac{dp(t)}{dt} \quad (\text{Eq. 2})$$

Where V is the volume of the lower chamber, L the thickness of the membrane, A is the effective area of the membrane interaction, T the absolute temperature, p_0 the pressure of the upper chamber and $dp(t)/dt$ the pressure increase rate in the lower chamber at the steady state. This value is the slope of the line that fits the linear section of pressure vs time plot. The measurement conditions were from 25 °C to 55 °C and pressures from 2 bar to 5 bar.

Apparent diffusion coefficient was obtained using the time lag model, θ , using the expression [20,21]:

$$D_a = \frac{L^2}{6\theta} \quad (\text{Eq. 3})$$

The θ value is obtained as the intersection of the above mentioned line with the time axis. Another important aspect is that gas separation selectivity is considered ideal and defined as [20,21] :

$$\alpha \left(\frac{A}{B} \right) = \alpha_{A/B} = \frac{P_A}{P_B} \quad (\text{Eq. 4})$$

Where, P_A and P_B are the permeation coefficients for gases A and B, respectively. Frequently the most permeable gas is taken as A, so that $\alpha_{A/B} > 1$.

2.10. Permeability to gases

O₂ permeability values were measured in dry conditions by using an Oxtran 2/20 (Mocon, Minneapolis as described earlier [22]. Permeability data for other gases were obtained by an isostatic method based on a permeation cell connected in series to a gas chromatograph (GC) equipped with a TCD detector as described elsewhere [22,23,24]. In brief, the film under analysis separates the two chambers of the permeation cell. In the low concentration chamber, a constant flow of helium (f) carries the permeated molecules out of the cell and to the injection valve of the GC. The high concentration gas on the high concentration chamber a constant flow of the permeant gas (or gas mixture) maintains the pressure of the gas constant at 1 atm (or 0.5 atm for gas mixtures). Gas pressures were adjusted by appropriate manometers and flows were controlled by needle valves and measured and mass flow meters from Dakota Instruments (New York). Gas samples of the He flow stream were injected until peak area got constant, indicating the achievement of stationary state. The GC response was previously calibrated by injection of known amounts of the tested gases. Permeability values were calculated from the concentration of the permeant at stationary state (c_∞) as follows:

$$P_i = \frac{c_\infty \cdot L}{f \cdot A \cdot \Delta p_i} \quad (\text{Eq. 5})$$

Where Δp_i is the pressure difference of gas “i” between the two chambers of the cell. Experiments were carried out in triplicate. Results shown are the mean values, the experimental error being estimated in 5%.

3. Results and discussion

ZIF powders were successfully obtained following the experimental procedure and then incorporated in the polymeric solution to obtain the membranes series PZIFs. *PZIFs membranes and the white polyetherimide membrane were studied; although the family of PZIFs membranes starts from the same polymeric base, same synthesis conditions, same concentrations and similar thicknesses ($100 \pm 18 \mu\text{m}$); these membranes only differ in the fillers used: Zn and Co monometallic zeolitic imidazolate frameworks (ZIF-8 and ZIF-67, respectively), in addition to the bimetallic composition Zn/Co (ZIF-Zn/Co), considered a solid solution. It should be mentioned that the crystalline ZIFs in question are isostructural to each other, so that the pore sizes of the structures are similar among them. [18] Therefore, we proposed that the variation of the permeation coefficients obtained not only depends on the ratio of pore size/kinetic diameter of the gas, but also on the factors such as the isotropy and anisotropy of the electrical charge that are present in each of the ZIFs structures and the dipole moment of the gas in question. It can be said that the network of Z-Zn/Co seen from the atomic level (unlike the Z-Zn and the Z-Co), presents an anisotropic environment of metallic cations Zn and Co, throughout its entire network; The alternating combination of these metals (with ionic radii of 0.074 nm and 0.063 nm, respectively), promotes the creation of micotensions and local dislocations (between the assembling metal and the binder) that result in an anisotropic behavior of the electric charge which aims to interact with the dipolar and/or quadrupole moment of the gaseous molecules. An example of the above can be seen in the permeation analysis which will be seen in detail later.*

3.1 Porosity analysis

In the Figure 1. shows the nitrogen sorption isotherms of the Z-Zn, Z-Co and Z-Zn/Co. The results indicate a reversible type I isotherm, characteristic of microporous materials. Porosity analysis of the ZIFs in question by means of isotherms of adsorption/desorption is

very relevant (especially Z-Zn/Co), because the Z-Zn/Co to be a solid solution (of the mixture bimetallic Zn and Co) and present an isostructural crystalline structure to that of Z-Zn and Z-Co, showed an intermediate surface area to that of its two predecessors (Z-Zn and Z-Co). The values of BET area and micropore volume are shown in the same figure:

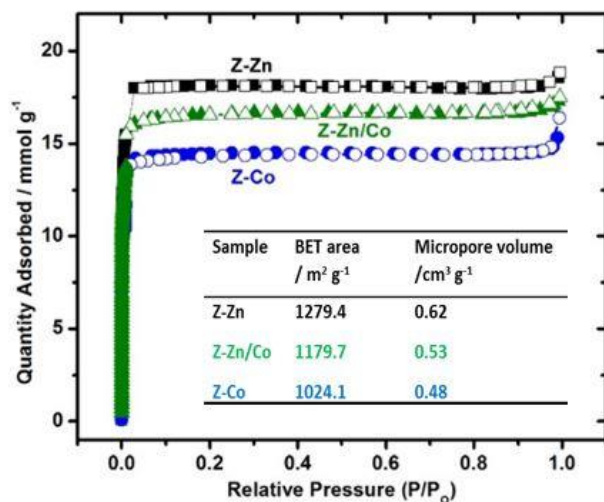


Figure 1. Isotherms of adsorption/desorption of the ZIFs. The closed marks refer to the N₂ adsorption measurements while the open marks refer to the desorption measurements.

3.2 Scanning electron microscopy

Micrographs of the Z-Zn filler and the PZ-Zn membranes are shown in Figure 2-a and 2-b, respectively. The increase in the concentration of fillers ZIFs in the polymeric base PEI if it affects the strength of the membranes of mixed matrix however it is possible to work without fracture problems using concentrations in 10 wt% and 20 wt%. Ma. Josephine and coworkers. [25] report the permeability of N₂, CH₄, and C₃H₈ in mixed matrix membranes (composed of matrimid/ZIF-8) in percent weight concentrations of ZIF-8, which they range from 0 wt% (polymeric base alone) to 60 wt%. The micrographs obtained from the as-synthesized Z-Zn powders exhibited well-defined crystallites and an average particle size of 2.6 μm (see Figure 2-a), bigger than particle size of the as-synthesized Z-Co and Z-Zn/Co powders (1.8 μm and 1.2 μm, respectively). On the other hand, a cross-section of the PZ-Zn membrane is shown in Figure 2-b, which exhibits a random dispersion of the particles in the PEI polymer base. Figure 2-c shows in greater detail the fracture and fragmentation of the ZIFs crystalline particles (with an average size has been reduced to 9 μm) located in the

polymeric matrix. The reduction of the ZIFs particles size and their morphological change of these fillers are associated with the exposure period of the colloidal solution in the ultrasonic bath. This change turned to be advantageous because the crystalline phase is still preserved, while the effective contact area to the permeating gases increases with the increase in the population of small particles well dispersed in the polymer phase.

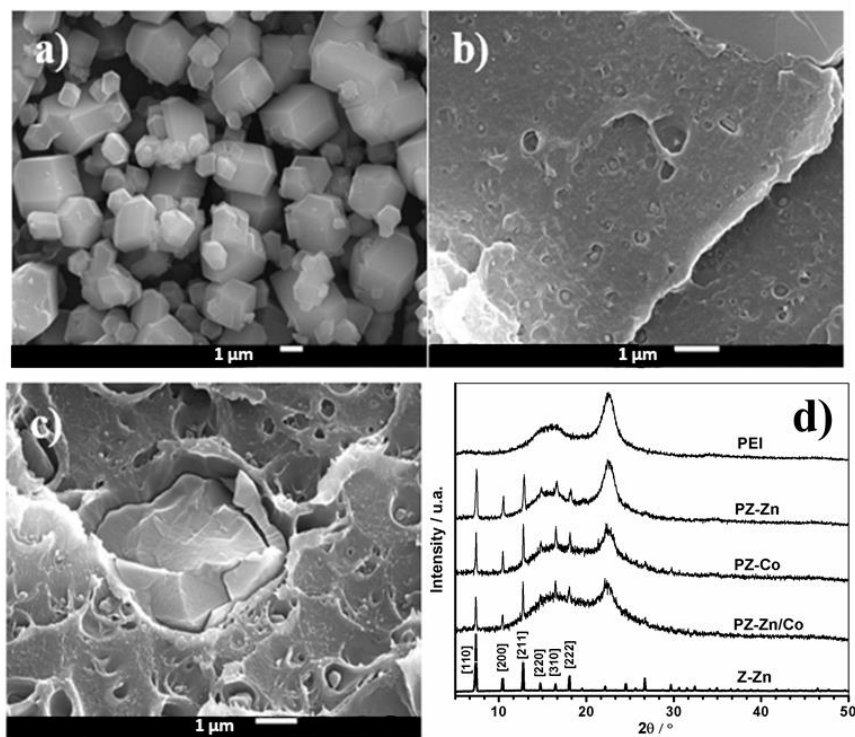


Figure 2. SEM micrographs and XRD patterns. a) Z-Zn, b) PZ-Zn/Co, c) Z-Zn/Co particles fractured inside of PEI and d) XRD patterns of membrane series and Z-Zn powder.

3.3. X-ray diffraction analysis

XRD patterns of the series of membranes and the phase of Z-Zn are shown in Figure 2-d and evidence the presence crystalline of the Z-Zn, Z-Co, and Z-Zn/Co incorporated into the PEI polymer base [8,26,17]. The crystalline phases of the obtained ZIF materials were identified using the "Match" program and using the Scherrer equation, the particle size was determined, which has the following trends: Z-Zn (1225 Å) > Z-Co (1120 Å) > Z-Zn/Co (879 Å). In the process of synthesis and self-assembly of the Z-Zn/Co, the tensions due to the mixture of metals (Zn/Co) and the organic linker may be a limiting factor for particle growth. [27]

Preliminarily in Figure 2-d it can be seen that the first diffraction maximums of the MMM (corresponding to the crystalline phase) are widened compared to the diffraction maximums of the Z-Zn sample; This behavior is attributed to finite dimensions of the crystallites, that is, the smaller the crystal, the more atoms will be out of optical coherence and consequently the diffraction maximums will widen. Subsequently, the particle size of the ZIFs fillers within the polymer matrix was determined resulting in smaller crystallites compared to the crystallites before the preparation of the colloid; The results obtained show the following trend: Z-Zn (966 Å) > Z-Co (941 Å) > Z-Zn/Co (796 Å).

3.4. Thermogravimetric analysis

The thermogravimetric curves of the PZIFs membranes are showed in the Figure 3. The curves presented a weight loss in the temperature range of 170 °C to 300 °C, later showed a constant weight profile up to 300 °C. This first weight loss was related to the evaporation of the solvent molecules trapped in the membranes (mainly in the polymeric matrix) and results in 5.4%, 6%, 7.2% and 8% losses for PEI, PZ-Zn, PZ-Co and PZ-Zn/Co, respectively. It is common to think that the solvent molecules trapped in the membranes could plasticized the matrix increasing the transport of gases and affecting the values of their representative coefficients (P_a and D_a) of the ternary system (polymer/ZIFs/solvent), although this is not our case. Using the PEI membrane as a reference, the permeability values obtained (which will be discussed later) were similar to those reported in the literature. Probably, the solvent molecules were removed during the activation time of the membranes (vacuum of 8 hours) to which they were submitted before each test. As Figure 3 shows, the weight of all PZIFs remained constant within the 300 °C-360°C range. At 360°C, the thermograms showed the initiation of a second weight loss which finished ca. 500°C, and that accounts for ca. 30% of the original sample weight. This loss could be related with the decomposition of the ZIFs materials. At higher temperatures, the curves showed a similar profile with a smooth slope which is related with the decomposition of the polymer.

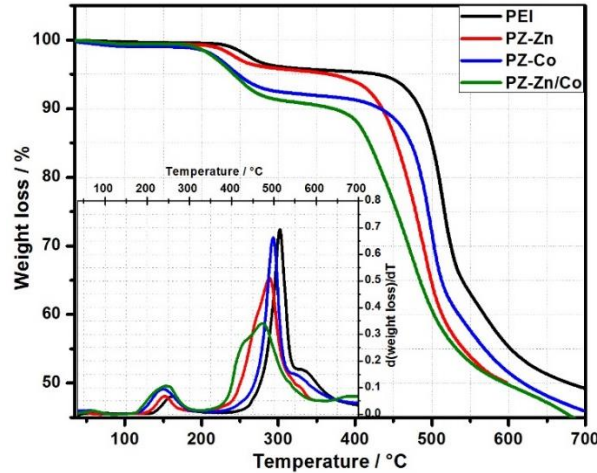


Figure 3. Thermogravimetric analysis of PEI and PZIFs membranes

3.5. Apparent gas permeation in PZIFs membranes

Figure 4 shows the permeability coefficients to CO₂ and N₂ for PEI and PZIFs at 35 °C and 2 bar conditions. To verify the correct operation and calibration of the permeation equipment, the PEI membrane was taken as a reference. The apparent permeability to CO₂ and selectivity of gases (CO₂ and N₂) in the PEI membrane, were $P_a = 1.25$ barrer and $\alpha_{P_a(CO_2)/P_a(N_2)} = 24.01$, respectively, similar to already reported data [28]. In the case of PZIFs membranes at 10 wt % concentration, the permeabilities were slightly lower than those obtained for the PEI membrane.

On the other hand, the series of membranes of greater concentration (20 wt %) showed different behaviors: The permeability coefficients for CO₂ obtained for the membrane series showed the following trend: PZ-Co > PZ-Zn > PEI > PZ-Zn/Co; while the permeability coefficients for N₂ showed the following trend: PZ-Co > PZ-Zn/Co > PEI > PZ-Zn. Although the fillers are at the same concentration, isostructural and with similar pore size (3.4 Å), the P_a to CO₂ for the membrane with PZ-Zn/Co filler was considerably lower. Similar behavior was observed for the rest of temperatures analyzed (see supporting information). This phenomenon could be attributed to intrinsic properties of the filler Z-Zn/Co (since the method of preparation and measurement conditions of the membrane series were the same). Such intrinsic properties should be reviewed in terms of isostructurality, pore size, crystallite size and local charge anisotropy.

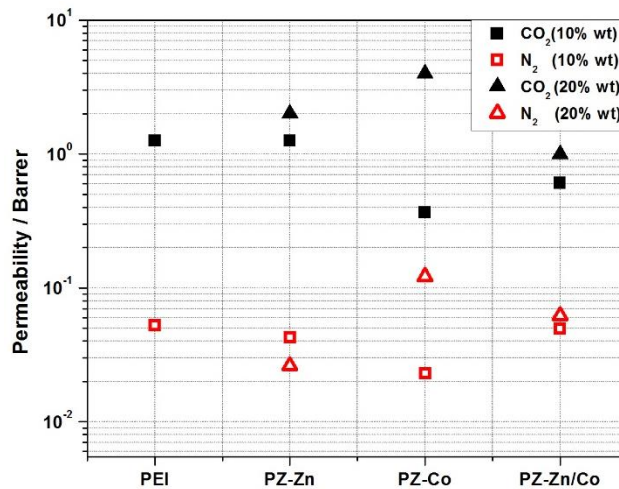


Figure 4. Graphics of permeability series membranes to 2 bar and 35°C

According to the results observed in the figure 4, it can be considered that the increase of the concentration of the fillers in the PEI polymer base has as consequence the increase of the permeability of the gases through the mixed matrix membrane (MMM), this is attributed to the increase of the contact surface crystallite-polymer. The crystallite-polymer interface present in the MMM can be considered as a number of preferential paths for the transport of gases. Therefore it could be said that, the higher the concentration of the filling, the greater the gas permeability, through these preferential roads; An important fact is that ZIFs are also known for their properties in gas sorption [29,30,31] so having a certain crystallite-polymer contact surface can reduce the permeability of gases and even more when the material counts with seductive properties (such as the anisotropy of electric charge that is present in the Z-Zn/Co material) that allow it to attract gaseous molecules. In addition, the particle size aims to be another critical factor that participates in the reduction of permeability to CO₂ in the membrane with PZ-Zn/Co filler. This filler has smaller crystallite sizes than Z-Zn and Z-Co providing greater effective contact area with the permeant gas. Electron density distribution is not-uniform due to the presence of the metallic cations (local charge anisotropy) and this leads to crystallites with more reduced dimension than in the monometallic ZIFs (Z-Zn and Z-Co). Smaller crystallites better dispersed in the polymer matrix result in larger interacting area for the permeant molecules. Subsequently, the P_a value decreased by half in the case PZ-Zn/Co while the P_a values for the other two ZIFs increased, what it is attributed to the absence of local charge anisotropy, bigger particle size (smaller contact area) and a slight increase in

pore size. The most important of the three factors is the local charge anisotropy since CO₂ molecules have a quadrupole moment of (-4.3 erg^{1/2} cm^{5/2} × 10²⁶) and a polarizability (2.9 × 10²⁴ cm³) that results in an effect on its permeability as a consequence of the contacting area composition [18].

The values of P_a and D_a for the developed membranes (obtained by “time-lag” method and with a measurement error of 3 %) are shown in Table 1. As it is known, the rapidity at which the mass transport of gaseous molecules occurs across a membrane depends mainly on the size of the kinetic diameter of the permeant gas, so it is usual for the permeation values to be higher for molecules with smaller kinetic diameter and smaller for those with greater kinetic diameter (for example: P_{CO₂} > P_{N₂}) [20]. The attractive interactions between molecules with quadrupole moment, Q, (such as Q_{N₂} (-1.5 erg^{1/2} cm^{5/2} × 10²⁶) and Q_{CO₂} (-4.3 erg^{1/2} cm^{5/2} × 10²⁶)), and the local electric field present in lattices ZIFs, are an example of the sorption force [18,32]. In the process of gas transport through the PZIFs, these sorption forces are present and are evidenced on the permeability values obtained (see Table 1).

Table 1

Values of apparent permeability and diffusion coefficients at 35 °C and p₀ = 2 bars.

Membrane	P _a / Barrer		D _a × 10 ⁻¹⁰ / cm ² s ⁻¹	
	CO ₂	N ₂	CO ₂	N ₂
PEI	1.25±0.08	0.052±0.002	25±2	25 ±2
PZ-Zn	1.79±0.09	0.031±0.001	44±3	30±3
PZ-Zn/Co	0.64±0.03	0.062±0.003	106±5	122±9
PZ-Co	3.33±0.17	0.120±0.006	35±2	20.3±1.7

Apparent selectivities, $\alpha_{P_a(CO_2)/P_a(N_2)}$, in the series of membranes are shown in Figure 5. The results obtained in the PZ-Zn hybrid membrane with 10% filler showed a slight improvement in the $\alpha_{P_a(CO_2)/P_a(N_2)}$ compared to the control PEI membrane, while that the PZ-Co and PZ-Zn/Co membranes with 10 wt% filler showed $\alpha_{P_a(CO_2)/P_a(N_2)}$ lower than PEI. The $\alpha_{P_a(CO_2)/P_a(N_2)}$ for the PZ-Zn and PZ-Co membranes in concentration 20 wt% of filler, showed greater selectivity than the PEI, while the PZ-Zn/Co membrane did not show a relevant change. It can be considered that the low $\alpha_{P_a(CO_2)/P_a(N_2)}$ of the PZ-Zn/Co membrane is mainly related to the retention of CO₂ due to the anisotropy of local charge present in the

filling, so it can be proposed that the permeability of CO₂ in the membrane (PZ-Zn/Co) is reduced by effects of a local field and the transport of N₂ by the pore size of the membrane. The series of membranes showed a similar behavior at all tested temperature and pressure conditions (see complementary material). Table 2 shows effect of temperature on the apparent permselectivity values obtained for the PZIFs membranes at 2 bar pressure.

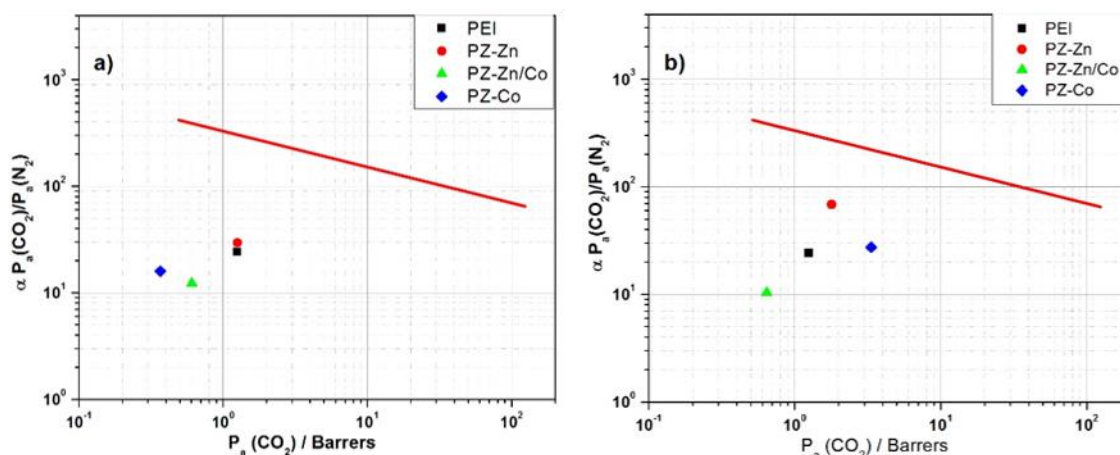


Figure 5. Apparent selectivity in PZIFs and PEI at 2 bar and 35°C: PZIFs with a) 10 wt % fillers and b) 20 wt % fillers

Table 2. Apparent selectivities to membrane white 20% wt at 2 bar.

T / °C	$\alpha_{P_a(CO_2)/P_a(N_2)}$			
	Sample			
	PEI	PZ-Zn	PZ-Zn/Co	PZ-Co
25	20.38±0.02	46.81±0.05	5.11±0.01	30.53±0.07
35	24.01±0.04	39.60±0.05	10.35±0.02	27.35±0.09
45	24.90±0.04	35.49±0.06	11.62±0.03	22.94±0.10
55	26.48±0.05	33.82±0.07	13.13±0.04	22.42±0.10

Samano and coworkers. [18] reported the separation of the H₂/CO₂ and CH₄/CO₂ binary mixtures using packed columns of ZIFs (ZIF-4, ZIF-8, ZIF-67 and ZIF-ZnCo). The gas separation study showed that the solid ZIF-Zn/Co solution exhibited higher sorption of molecules with quadrupole moment (for example H₂ and CO₂) compared to their analogues. The chromatographic profile of Figure 6 shows the response times of the CH₄/CO₂ binary mixture using a column packed with PZ-Zn/Co fillers at a concentration of 10 wt% and a temperature at 30 °C; the results of this study showed shorter response times compared to those obtained in a column packed with ZIF-ZnCo powders (5 times smaller) previously

reported [13]. The separation behavior for the gas mixture CH₄/CO₂ in the column with PZ-Zn/Co gaskets (similar to the behavior of ZIF-ZnCo) supports the hypothesis of CO₂ sorption in local sites of the PZ-Zn/Co membrane, explaining the reduction of selectivity when using gases with relatively large kinetic diameters and molecules with quadrupole moments.

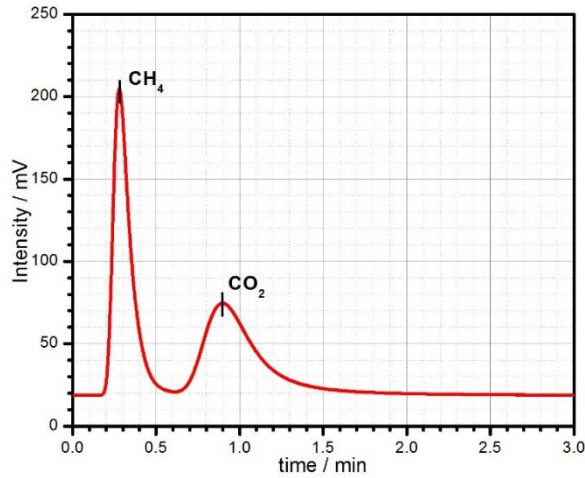


Figure 6. Chromatogram of separation CH₄/CO₂ in PZ-Zn/Co

Assuming that the gas transport processes through these membranes are thermally activated, the activation energy values can be calculated using the Arrhenius equation:

$$X = X_0 \exp\left(\frac{-E_X}{RT}\right) \quad \text{Eq. 6}$$

where X stands for apparent of permeation or diffusion coefficient (P_a and D_a), X_0 corresponds to the pre-exponential factor and E_X to the activation energy of P_a or D_a . Arrhenius plots of P_a and D_a to CO₂ and N₂ for the PEI and PZIFs membranes at 2 bars are shown in Figure 7 and the calculated activation energy values are included in Table 3. The activation energies associated with CO₂ permeation coefficients in the membranes decreased in the order: PZ-Zn/Co > PEI > PZ-Zn > PZ-Co, at 2 bars. The activation energies for N₂ in the series of membranes showed less variation compared to CO₂, although the values obtained can also be ordered as: PZ-Zn > PZ-Zn/Co > PEI > PZ-Co in the third column of Table 3. The values of the apparent sorption enthalpies of CO₂ and N₂, ($\Delta H_s = E_P - E_D$), are also shown in Table 3. It is noticeable that the sorption enthalpy values calculated for the PZIFs are of the same order than those obtained for the fillings in their single phase [18]. These values indicate that the solubility processes of CO₂ in PEI membrane and hybrid

membranes with fillers Z-Zn and Z-Co are exothermic. On the contrary, for membranes with Z-Zn/Co the sorption processes for CO₂ and N₂ are endothermic.

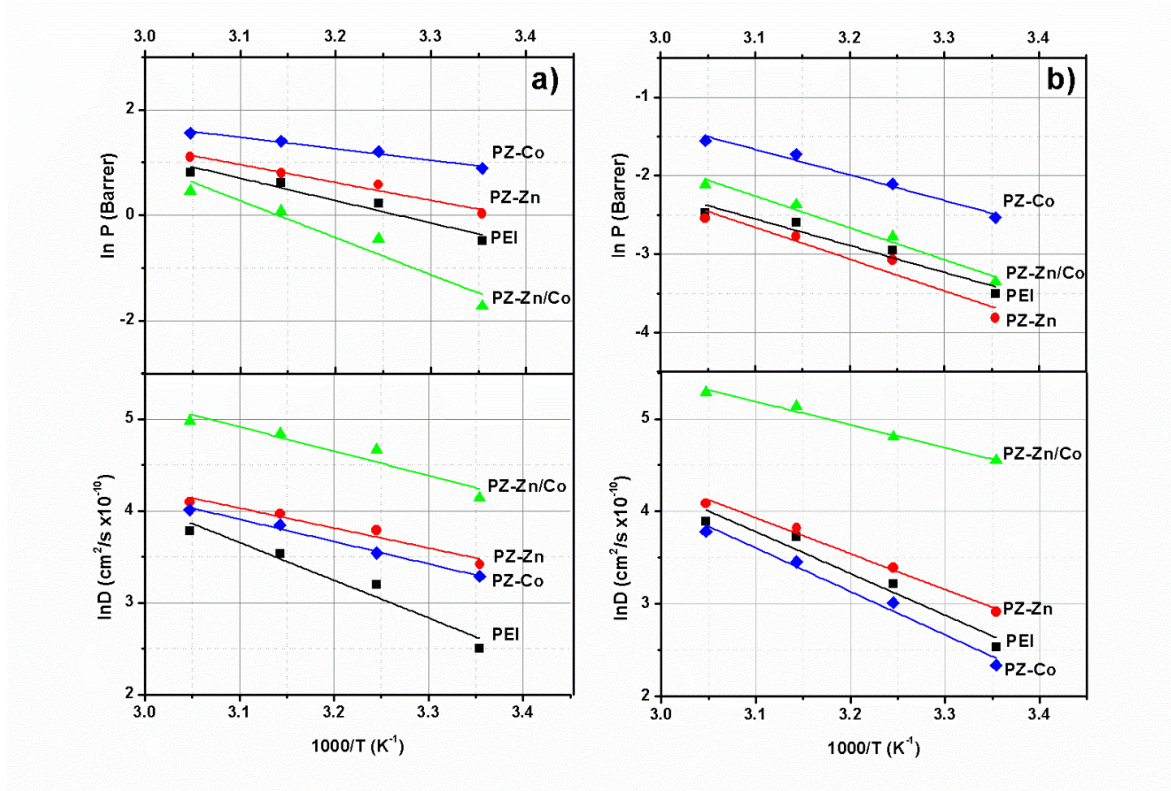


Figure 7. Arrhenius for apparent permeability and diffusion of a) CO₂, b) N₂, at 2 bars.
Color symbol Black, Red, Green, and blue corresponding to PEI, PZ-Zn, PZ-Zn/Co and PZ-Co

Note that the enthalpy of sorption of CO₂ in the PZ-Zn/Co membrane is greater than that of its analogues (PZ-Zn and PZ-Co), which supports the low selectivity obtained $\alpha_{P_a(\text{CO}_2)/P_a(\text{N}_2)}$ due to the adsorption of CO₂ within the membrane and the possible obstruction of gaseous molecules through the hybrid membrane.

Table 3

Activation energy (E_a) of the permeation and diffusion processes and sorption enthalpy for CO₂ and N₂ in the diverse tested membranes at 2 bar.

Films	$E_P / \text{kJ mol}^{-1}$		$E_D / \text{kJ mol}^{-1}$		$\Delta H_s / \text{kJ mol}^{-1}$	
	CO ₂	N ₂	CO ₂	N ₂	CO ₂	N ₂
PEI	32.8 ± 1.8	31.0 ± 0.3	36.0 ± 0.3	37.4 ± 0.3	-3.2 ± 2.1	-6.4 ± 0.6
PZ-Zn	17.6 ± 1.3	36.9 ± 0.3	18.1 ± 0.3	30.5 ± 0.3	-0.6 ± 1.6	6.4 ± 0.6
PZ-Zn/Co	58.1 ± 1.1	33.8 ± 0.4	22.1 ± 0.2	20.7 ± 0.2	36.0 ± 1.3	13.0 ± 0.6
PZ-Co	18.0 ± 0.8	27.0 ± 0.5	20.2 ± 0.3	43.8 ± 0.3	-2.1 ± 1.1	-16.8 ± 0.8

3.6. Gas mixture study

The estimation of permeability to single and mixture of gases at atmospheric pressure through PEI and PZIFs at 10% ZIF weight concentration was carried out by an isostatic method described in the experimental section. Figure 8 shows the apparent permeability values (of the individual gases O₂, CO₂, and CH₄) and the permselectivity of the gas pairs. In Figure 8-a, it can be observed that in all membranes, CO₂ is the most permeable gas of the three tested, followed by O₂ and CH₄, as it could be expected from reported data in other polymers. The greater solubility of CO₂ caused by its condensability is mainly responsible for the high P values. A comparison between membranes shows that PEI offers an intermediate barrier to all these three gases than PZ-Zn (higher) and PZ-Co (lower).

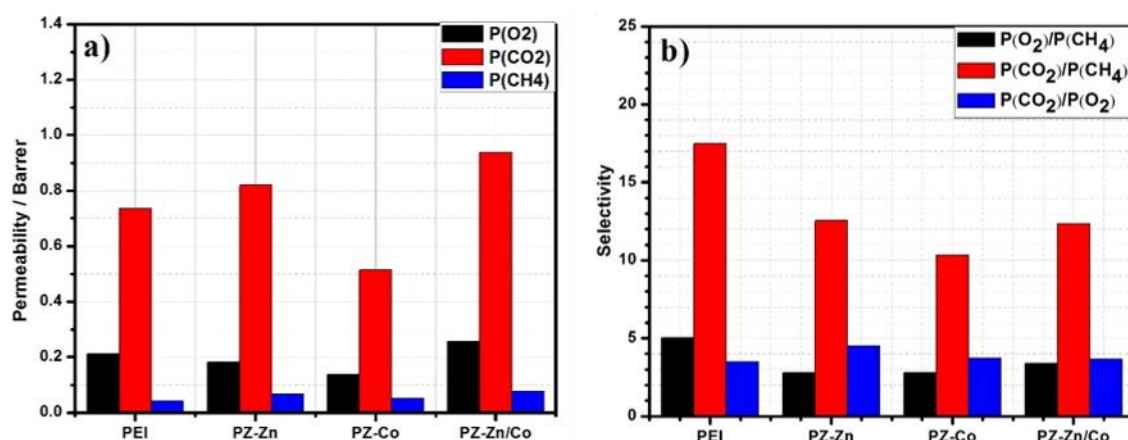


Figure 8. Values of the permeability coefficients of single gas in PEI and PZIFs membranes (plot a) and apparent selectivity (plot b) measured at room temperature and at 1 atm of pressure.

After these results, one could expect that the P_a values for the PZ-Zn / Co membrane would be intermediate to those with the single metallic ZIFs (PZ-Zn and PZ-Co), however the permeability coefficients of O₂, CO₂ and CH₄ in the PZ-Zn / Co are larger showing that the Z-Zn/Co filling is a solid solution and its behavior is typical of a new material with different properties than the Z-Zn and Z-Co.

From the values of apparent permeability (see Table 4) the permselectivity of the membranes for the diverse gas pairs were calculated and are also presented in Figure 8-b. In general, the results obtained for the PZIFs membranes showed low selectivities compared to the PEI as blank; however, it is important to mention that the selectivity behavior of the membrane series preserves a pattern similar to the selectivities shown in Figure 5-a. The relationship of

the observed pattern (by the variable-volume pressure-constant method and isostatic method) allows us to suggest that the concentration in percent weight of the PZIFs membranes is a potential factor for the increase of selectivity of the gases in question.

Table 4

Permeability and selectivity of single gases at conditions of 1 atm and room temperature.

Sample	$P_a \times 10^{-1}$	$P_a \times 10^{-1}$	$P_a \times 10^{-2}$	$P(O_2)/P(CH_4)$	$P(CO_2)/P(CH_4)$	$P(CO_2)/P(O_2)$
	(O_2)	(CO_2)	(CH_4)			
	<i>Barrer</i>					
PEI	2.1±0.1	7.4±0.4	4.2±0.2	5.0±0.5	17.5±1.8	3.5±0.4
PZ-Zn	1.8±0.1	8.2±0.4	6.6±0.3	2.8±0.3	12.5±1.2	4.5±0.5
PZ-Co	1.4±0.1	5.1±0.3	5.0±0.2	2.8±0.3	10.4±1.0	3.7±0.4
PZ-Zn/Co	2.6±0.1	9.4±0.5	7.6±0.4	3.4±0.3	12.3±1.3	3.7±0.4

Figure 9 shows the gas permeability measured by the isostatic method with two gas mixtures, CO_2/CH_4 and CH_4/C_2H_4 .

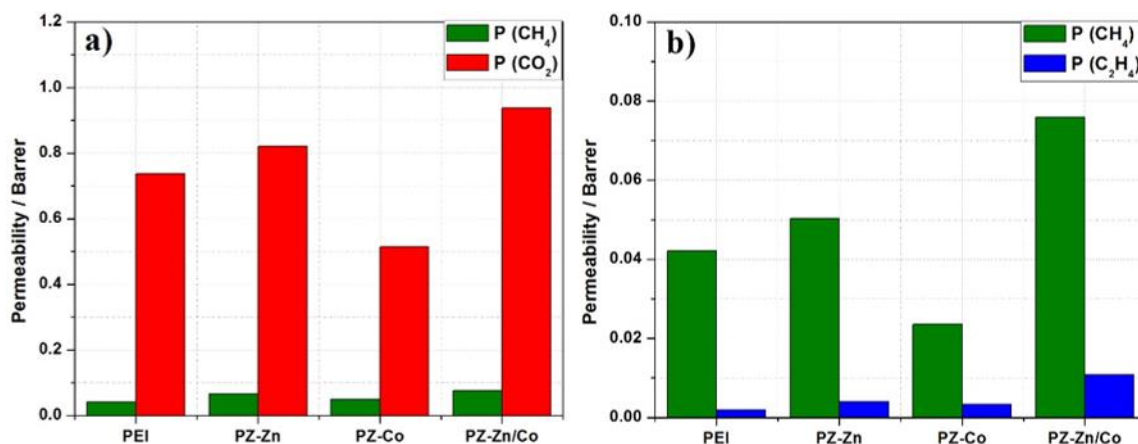


Figure 9. Graphics of a) permeation of mixture gases (CO_2/CH_4) in membrane series and b) selectivity of mixture gases (CH_4/C_2H_4) in membrane series, both at room temperature and 1 atm of pressure.

Similar to the apparent permeation of single gases, the transport values of these gas mixtures through the PZIFs membranes were higher (with the exception of the PZ-Co membrane) than through PEI membrane. In the case of the CO_2/CH_4 mixture (see Figure 9-a) the permeation values obtained for CO_2 are in the $5.13 \times 10^{-1} - 9.37 \times 10^{-1}$ barrer range, while that for CH_4 , are in the 4.21×10^{-2} to 7.59×10^{-2} barrer range. The transport is slower for CH_4 than for CO_2 , in agreement with reported literature values and suggests that the transport of gases through the PZIFs and PEI membranes is mainly due to the kinetic diameter of the species in question (0.38 nm for CH_4 and 0.33 nm for CO_2). This considerations is also valid for the CH_4/C_2H_4

mixture. As can be observed in Figure 9-b the permeabilities of CH₄ are greater than those of C₂H₄ (with kinetic diameters of 0.38 and 0.39, respectively). [20] Comparing between membranes, a similar profile to those observed for pure gases and mixtures were obtained. The PZ-Zn/Co membrane presented the greatest permeabilities followed by PZ-Zn, and PEI, and again the PZ-Co showed the greatest barrier properties.

Table 5. Permeability and selectivity values of mixture gases at 1 atm and room temperature.

Sample	CO ₂ /CH ₄			CH ₄ /C ₂ H ₄		
	Px10 ⁻² (CH ₄)	Px10 ⁻¹ (CO ₂)	α (CO ₂ /CH ₄)	Px10 ⁻² (CH ₄)	Px10 ⁻³ (C ₂ H ₄)	α (CH ₄ /C ₂ H ₄)
	<i>Barrer</i>			<i>Barrer</i>		
PEI	4.21±0.21	7.36±0.37	17.49±0.30	4.21±0.21	1.85±0.09	22.73±0.15
PZ-Zn	6.55±0.30	8.20±0.41	12.53±0.40	5.02±0.25	4.04±0.20	12.44±0.20
PZ-Co	4.97±0.25	5.13±0.26	10.34±0.40	2.35±0.12	3.36±0.17	7.00±0.20
PZ-Zn/Co	7.59±0.38	9.37±0.47	12.34±0.42	7.59±0.38	1.09±0.05	6.99±0.22

Table 5 presents the permeability of the mixtures and the permselectivities calculated from the P values. The selectivities determined for both gas mixtures (CO₂/CH₄ and CH₄/C₂H₄) in the series of membranes showed that the polymer base PEI presents a greater gas discrimination compared to the hybrid membranes with 10% ZIF weight concentration. Nevertheless, we suggest that the selectivity of PZIFs can change with ZIF concentration according to the results obtained with the variable-volume pressure-constant method.

4. Conclusions

The series of membranes obtained had regular thicknesses (100 ± 18 μm) and free of defects; They also exhibited good flexibility during the assembly process and did not present ruptures or breaking points during the permeation process.

In this work, single gas permeation values of CO₂ and N₂, through PEI membranes containing ZIFs at 10% and 20% weight were measured by the "time-lag" method. In addition, the permeation values of single gases (O₂, CO₂ and CH₄) and gas mixtures (CO₂/CH₄ and CH₄/C₂H₄) through PZIFs membranes with 10% of ZIF were obtained by an "isostatic" procedure at atmospheric pressure. The PZIFs with fillers of Z-Zn and Z-Co showed apparent selectivities ($\alpha_{P_a(CO_2)/P_a(N_2)}$) of 39.6 and 27.5 respectively, higher than the $\alpha_{P_a(CO_2)/P_a(N_2)}$

of the PEI membrane, while the membrane with the bimetallic ZIF (PZ-Zn/Co) showed the lowest $\alpha_{P_a(CO_2)/P_a(N_2)}$ selectivity (10.3) of the membrane series (under conditions of 25 °C and 2 bar). It is proposed that the selectivity of the membrane series can be attributed to two critical factors: the particle size/distribution ratio in the polymer base and sorption of CO₂ at local sites of the bimetallic mixture

The permeability values for the PZIFs vary with respect to the concentration of the filler and the adsorbate-adsorbent ratio. The results obtained in the PZ-Zn hybrid membrane with 10% filler weight showed a slight increase in the $\alpha_{P_a(CO_2)/P_a(N_2)}$ while that the PZ-Co and PZ-Zn/Co membranes with 10 wt% filler showed $\alpha_{P_a(CO_2)/P_a(N_2)}$ lower than the PEI control membrane, The selectivity of CO₂ in membranes of concentration 10% wt of ZIFs was lower than the PEI however, when doubling the concentration (20% wt of ZIFs) the increase in selectivity was observed only for the PZ-Zn and PZ-Co membranes.

The activation energy calculated using Arrhenius expression in the activated state theory shows activation energies associated with CO₂ permeation coefficients in the membranes were reducing in the order PZ-Zn/Co > PEI > PZ-Zn > PZ-Co, at 2 bars. However the activation energies for N₂ showed less variation compared to CO₂. The values of the apparent sorption enthalpies of CO₂ and N₂, presented by the PZIFs is of the same order as the fillings in its single phase. The results indicate that heats solubility CO₂ in PEI and hybrid membranes with fillers Z-Zn and Z-Co are exothermic processes. For filling the membrane with Z-Zn/Co heats of solubility of CO₂ and N₂ are endothermic processes.

Acknowledgment

This research has been supported by the ENE/2015-69203-R project, granted by the Ministerio de Economía y Competitividad (MINECO), Spain; Also authors are grateful to UNAM-DGAPA-PAPIIT projects IG-100185, and IG-114818.

This study was partially supported by the CONACyT (Mexico) projects 2013-05-231461 and CB-2014-01-235840.

The authors appreciate the access to the experimental facility of the National Laboratory for Energy Conversion and Storage (CONACyT) to carry out the experimental study.

References

- 1 P. Bernardo, E. Drioli and G. Golemme. Membrane Gas Separation: A Review/State of the Art. *Ind. Eng. Chem. Res.*, 48 (10) (2009), 4638. <https://doi.org/10.1021/ie8019032>.
- 2 W. Yave, M. G. Buonomenna and G. Golemme. Some approaches for high performance polymer based membranes for gas separation: block copolymers, carbon molecular sieves and mixed matrix membranes. *RSC Advances*, 2 (2012), 10745. <https://doi.org/10.1039/C2RA20748F>
- 3 A. W. Thornton, D. Dubbeldam, M. S. Liu, B. P. Ladewig, A. J. Hilla and M. R. Hill. Feasibility of zeolitic imidazolate framework membranes for clean energy applications. *Energy & Environmental Science*, 5 (2012), 7637. <https://doi.org/10.1039/C2EE21743K>
- 4 Y. Zhang, J. Sunarso, S. Liu, R. Wang. Current status and development of membranes for CO₂/CH₄ separation: A review. *International Journal of Greenhouse Gas Control*, 12 (2013), 84. <https://doi.org/10.1016/j.ijggc.2012.10.009>
- 5 Y. Li, G. He, S. Wang, S. Yu, F. Pan, H. Wu and Z. Jiang. Recent advances in the fabrication of advanced composite membranes. *Royal Society of chemistry*, 1 (2013), 10058. <https://doi.org/10.1039/C3TA01652H>.
- 6 Troughton, M. J. *Handbook of Plastics Joining: A Practical Guide*. Elsevier Inc, 2008.
- 7 H. Farong, W. Xueqiu & L. Shijin. The Thermal Stability of Polyetherimide. *Polymer Degradation and Stability*, 18 (1987), 247. [https://doi.org/10.1016/0141-3910\(87\)90005-X](https://doi.org/10.1016/0141-3910(87)90005-X).
- 8 V. Guerrero, H. Jeong and M. McCarthy. Synthesis of Zeolitic Imidazolate Framework Films and Membranes with Controlled Microstructures. *Langmuir*, 18, 26 (2010), 14636. <https://doi.org/10.1021/la102409e>.
- 9 N. Stock, S. Biswas. Synthesis of Metal-Organic Frameworks (MOFs): Routes to Various MOF Topologies, Morphologies, and Composites. *American Chemical Society*, 112 (2012), 93. <https://doi.org/10.1021/cr200304e>.
- 10 G. Liu, V. Chernikova, Y. Liu, K. Zhang, Y. Belmabkhout, O. Shekhah, C. Zhang, S. Yi, M. Eddaoudi and W. J. Koros. Mixed matrix formulations with MOF molecular sieving for key energy-intensive separations. *Nature materials*, 17 (2018), 283. <https://doi.org/10.1038/s41563-017-0013-1>.
- 11 S. Yu, S. Li, S. Huang, Z. Zeng, S. Cui, Y. Liu. Covalently bonded zeolitic imidazolate frameworks and polymers with enhanced compatibility in thin film nanocomposite membranes for gas separation. *Journal of Membrane Science*, 540 (017), 155. <https://doi.org/10.1016/j.memsci.2017.06.047>.
- 12 Keskin, E. Atci and S. Atomically detailed models for transport of gas mixtures in ZIF membranes and ZIF/polymer composite membranes. *Industrial and Engineering Chemistry Research*, 51, 7 (2012), 3091. <https://doi.org/10.1021/ie202530f>.
- 13 L. Xiang, L. Sheng, C. Wang, L. Zhang, Y. Pan and Y. Li. Amino-Functionalized ZIF-7 Nanocrystals: Improved Intrinsic Separation Ability and Interfacial Compatibility in MixedMatrix Membranes for CO₂/CH₄ Separation. *Advanced Materials*, 29 (2017), 1606999. <https://doi.org/10.1002/adma.201606999>.
- 14 H. Wang, L. Zhao, W. Xu, S. Wang, Q. Ding, X. Lu, W. Guo. The properties of the bonding between CO and ZIF-8 structures: a density functional theory study. *Theor Chem Acc*, 134 (2015), 31. <https://doi.org/10.1007/s00214-015-1636-4>.

- 15 H. Huang, W. Zhang, D. Liu, B. Liu, G. Chen and C. Zhong. Effect of temperature on gas adsorption and separation in ZIF-8: A combined experimental and molecular simulation study. *Chemical Engineering Science*, 66 (2011), 6297. <https://doi.org/10.1016/j.ces.2011.09.009>.
- 16 K. Y. A. Lin, H. A. Chang. Ultra-High Adsorption Capacity of Zeolitic Imidazole Framework-67 (ZIF-67) for Removal of Malachite Green From Water. *Chemosphere*, 139 (2015), 624. <https://doi.org/10.1016/j.chemosphere.2015.01.041>.
- 17 R. Banerjee, A. Phan, B. Wang, C. Knobler, O. M. Yaghi. High-throughput synthesis of zeolitic imidazolate frameworks and application to CO₂ capture. *Science*, 319 (2008), 939. <https://doi.org/10.1126/science.1152516>.
- 18 C. Sámano, R. Cabrera, J. Hernández, A. Lemus, E. Reguera. Separation of H₂-CO₂ and CH₄-CO₂ binary mixtures by zeolite-like imidazolate frameworks. *Surfaces and Interfaces*, 5 (2016), 55. <https://doi.org/10.1016/j.surfin.2016.09.009>.
- 19 Standard Test Method for Determining Gas Permeability Characteristics of Plastic Film and Sheeting. *ASTM International* (2009).
- 20 Y. Yampolskii, I. Pinnau and B. Freeman. *Materials Science of Membranes for Gas and Vapor Separation*. John Wiley & Sons Ltd, 2006.
- 21 J. Villaluenga, B. Seoane and V. Compañ. Diffusional characteristics of coextruded linear low-density polyethylenes prepared from different conditions of processing. *Journal of Applied Polymer Science*, 70 (1998), 25. [https://doi.org/10.1002/\(SICI\)1097-4628\(19981003\)70:1<23::AID-APP5>3.0.CO;2-W](https://doi.org/10.1002/(SICI)1097-4628(19981003)70:1<23::AID-APP5>3.0.CO;2-W).
- 22 P. Cerisuelo, A. Alonso, S. Aucejo, R. Gavara and P. Hernandez. Modifications induced by the addition of a nanoclay in the functional and active properties of an EVOH film containing carvacrol for food packaging. *Journal of Membrane Science*, 423–424 (2012), 447. <https://doi.org/10.1016/j.memsci.2012.08.021>.
- 23 R. Gavara, R. Catala, P.M. Hernandez-Munoz, R.J. Hernandez. Evaluation of permeability through permeation experiments: isostatic and quasiisostatic methods compared. *Packaging technology & science*, 9 (1996), 215. [https://doi.org/10.1002/\(SICI\)1099-1522\(199607\)9:4<215::AID-PTS366>3.0.CO;2-U](https://doi.org/10.1002/(SICI)1099-1522(199607)9:4<215::AID-PTS366>3.0.CO;2-U)
- 24 ASTM D3985 - 05, Standard Test Method for Oxygen Gas Transmission Rate Through Plastic Film and Sheeting Using a Coulometric Sensor. *ASTM International, West Conshohocken, PA*. (2010).
- 25 Ma. Josephine, C. Ordoñez, K. J. Balkus Jr., J. P. Ferraris, I. H. Musselman. Molecular sieving realized with ZIF-8/Matrimid® mixed-matrix membranes. *Journal of Membrane Science* 361, 361 (2010), 28. <https://doi.org/10.1016/j.memsci.2010.06.017>.
- 26 C. Samano, J. Hernández, R. Cabrera, J.A.I. Díaz and E. Reguera. Tuning the adsorption potential. Separation of aromatic hydrocarbons by cobalt and zinc zeolitic imidazolate frameworks. *Colloids and Surfaces A: Physicochemical and Engineering Aspects*, 506 (2016), 50. <https://doi.org/10.1016/j.colsurfa.2016.06.008>.
- 27 Cublity, B. D. *Elements of X-ray diffraction*. ADDISON-WESLEY PUBLISHING COMPANY, INC., 1956.
- 28 Y. Dai, J.R. Johnson, O. Karvan, D. S. Sholl, W.J. Koros. Ultem®/ZIF-8 mixed matrix hollow fiber membranes for CO₂/N₂ separations. *Journal of Membrane Science*, 401-401 (2012), 76. <https://doi.org/10.1016/j.memsci.2012.01.044>.

- 29 L. Hertäg, H. Bux, J. Caro, C. Chmelik, T. Remsungnen, M. Knauth and S. Fritzsche. Diffusion of CH₄ and H₂ in ZIF-8. *Journal of Membrane Science*, 377 (2011), 36. <https://doi.org/10.1016/j.memsci.2011.01.019>
- 30 C. Chmelik, J. van Baten and R. Krishna. Hindering effects in diffusion of CO₂/CH₄ mixtures in ZIF-8 crystals. *Journal of Membrane Science*, 397–398 (2012), 87. <https://doi.org/10.1016/j.memsci.2012.01.013>
- 31 J. Li, J. Sculley, and H. Zhou. Metal–Organic Frameworks for Separations. *American Chemical Society*, 112 (2012), 869. <https://doi.org/10.1021/cr200190s>
- 32 Yang, R. *Adsorbents: Fundamentals and applications*. Wiley-Interscience, 2003.
- 33 H. Lin, L. Pei and C. T. Shung. PIM-1 as an organic filler to enhance the gas separation performance of Ultem polyetherimide. *Journal of Membrane Science*, 453 (2014), 614. <https://doi.org/10.1016/j.memsci.2013.11.045>.
- 34 V. Compañ, L. F. Del Castillo, S.I. Hernández, M. López and E. Riande. On the crystallinity effect on the gas sorption in semicrystalline linear low density polyethylene (LLDPE). *Journal of Polymer Science. Part B: Polymer Physics*, 45 (2007), 1798. <https://doi.org/10.1002/polb.21228>.